

Supplementary Materials

to accompany

First-Principles study of Photovoltaics and Carrier Mobility for Non-toxic Halide Perovskite $\text{CH}_3\text{NH}_3\text{SnCl}_3$: Theoretical Prediction.

by

Lin-Zhi Wang¹, Yu-Qing Zhao¹, Biao Liu¹, Li-Juan Wu¹, Meng-Qiu Cai^{1,2*}

¹School of Physics and electronics Science, Hunan University, Changsha, Hunan 410082, China

²Synergetic Innovation Center for Quantum Effects and Applications (SICQEA), Hunan Normal University, Changsha 410081, China

Supporting Information Placeholder

* Corresponding author. Tel.: +86 731 88821177.
E-mail address: mqcai@hnu.edu.cn (M.Q. Cai)

1 Details and methods

First-principles electronic structure calculations have been performed by the density function theory method (DFT), with the PBE type of the generalized gradient approximation to describe the exchange-correction functional.¹ The DFT calculations were performed by applying the Vienna Ab initio Simulation Package(VASP) code.^{2,3} For the exchange-correlation functional, the generalized gradient approximation (GGA) of Perdew-Burke-Ernzerhof(PBE)¹ is used to relax the structural parameters and to calculate the effective masses, optical properties and carrier mobility. Electronic orbitals 4d5s5p, 3s3p, 2s2p,2s2p, and 1s were considered in valence for Sn, Cl, C, N, and H atoms, respectively. The projector augmented-wave (PAW) pseudopotentials⁴ are used with an energy cutoff of 500eV for the plane-wave basis functions. The Monkhorst-Pack K-point mesh⁵ of 4*4*4 is employed in the structural optimization and is further increased to 8*8*8 in calculating the optical properties and carrier mobility. All the structures considered in this study were relaxed with conjugate-gradient algorithm until the energy on the atoms was less than 1.0×10^{-4} eV. There is no little effect on the results while increasing the k-points and the energy cutoff.

2 Lattice parameters of CH₃NH₃SnCl₃

We show the optimized lattice constants of cubic, monoclinic and triclinic CH₃NH₃SnCl₃ in Table S1. The computed values are compared with the experimental results. Theoretical structural results are a little larger than the experimental data

obtained in this work as well as with those reported by Yamada *et al.*⁶

	This work (Error!)			Experiment (Error!)		
	a	b	c	a	b	c
Cubic	5.90	—	—	5.76	—	—
Monoclinic	5.81	8.36	8.02	5.72	8.23	7.93
Triclinic	5.92	8.38	8.19	5.73	8.23	7.91

Table S1. Calculated Cell Parameters of $\text{CH}_3\text{NH}_3\text{SnCl}_3$ for cubic, monoclinic and triclinic phases with PBE along the Nonlocal Density Function (vdW-DF). Compared with Corresponding Experimental Results.⁶

3 The atomic position of C, N, Sn, and Cl elements of $\text{CH}_3\text{NH}_3\text{SnCl}_3$

Table S2: The atomic position of Sn, Cl, C, and N elements in cubic structure

		x	y	z	Occupation	site
1	Sn1	0.99313	0.06422	0.98873	1	1a
2	Cl1	0.54873	0.08706	0.00761	1	1a
3	Cl2	0.02587	0.48896	0.93710	1	1a
4	Cl3	0.99878	0.09651	0.43117	1	1a
5	C1	0.49732	0.59850	0.50521	1	1a
6	N1	0.48637	0.34678	0.52746	1	1a

Table S3: The atomic position of C, N, Sn and Cl elements in monoclinic structure

		x	y	z	Occupation	site
1	C1	0.63490	0.62858	0.40858	1	1a
2	C2	0.63490	0.37142	0.90758	1	1a
3	N1	0.68792	0.23183	0.32658	1	1a
4	N2	0.68792	0.76817	0.82658	1	1a
5	Sn1	0.68390	0.15378	0.01573	1	1a
6	Sn2	0.68390	0.84622	0.51573	1	1a
7	Cl1	0.18272	0.86978	0.12767	1	1a
8	Cl2	0.18272	0.13022	0.62767	1	1a
9	Cl3	0.89760	0.55763	0.28538	1	1a
10	Cl4	0.89760	0.44237	0.78538	1	1a

11	Cl5	0.17883	0.20828	0.10732	1	1a
12	Cl6	0.17883	0.79172	0.60732	1	1a

Table S4: The atomic position of N, C, Sn and Cl elements in triclinic structure

		x	y	z	Occupation	site
1	N1	0.82461	0.03923	-0.01014	1	1a
2	N2	0.96538	0.60737	0.58453	1	1a
3	C1	0.04825	0.95080	0.02711	1	1a
4	C2	0.97384	0.44281	0.50464	1	1a
5	Sn1	0.48985	0.50175	0.02715	1	1a
6	Sn2	0.44721	0.00830	0.51174	1	1a
7	Cl1	0.49154	0.22170	0.26773	1	1a
8	Cl2	0.89275	0.00166	0.57188	1	1a
9	Cl3	0.91863	0.44078	0.97109	1	1a
10	Cl4	0.61652	0.72855	0.24673	1	1a
11	Cl5	0.41925	0.21720	0.75264	1	1a
12	Cl6	0.47716	0.72292	0.77248	1	1a

4 dielectric response functions and the deformation potential (DP) of $\text{CH}_3\text{NH}_3\text{SnCl}_3$

The dynamical dielectric response functions of cubic, monoclinic and triclinic $\text{CH}_3\text{NH}_3\text{SnCl}_3$ were calculated by the First-Principle with vdW-DF in this work. They are more or less similar to each other. The black and red lines represent real and imaginary parts of the dielectric function $\varepsilon(\omega)$. The explicit expressions are given by

$$\varepsilon(\omega) = \varepsilon_1(\omega) + i\varepsilon_2(\omega), \quad (4)$$

From cubic to triclinic phase, for zero photon frequency, the imaginary part is 0 while the static dielectric constant is 2 to 3. As the structures are isotropic, all the diagonal components of $\varepsilon_1(\omega)$ and $\varepsilon_2(\omega)$ are identical. We found that the triclinic phase have the best optical properties compared to other two phases. Besides, they are **non-toxic** compared to the Pb-based materials. Therefore, the $\text{CH}_3\text{NH}_3\text{SnCl}_3$ is convenient to be used as solar-cell materials.

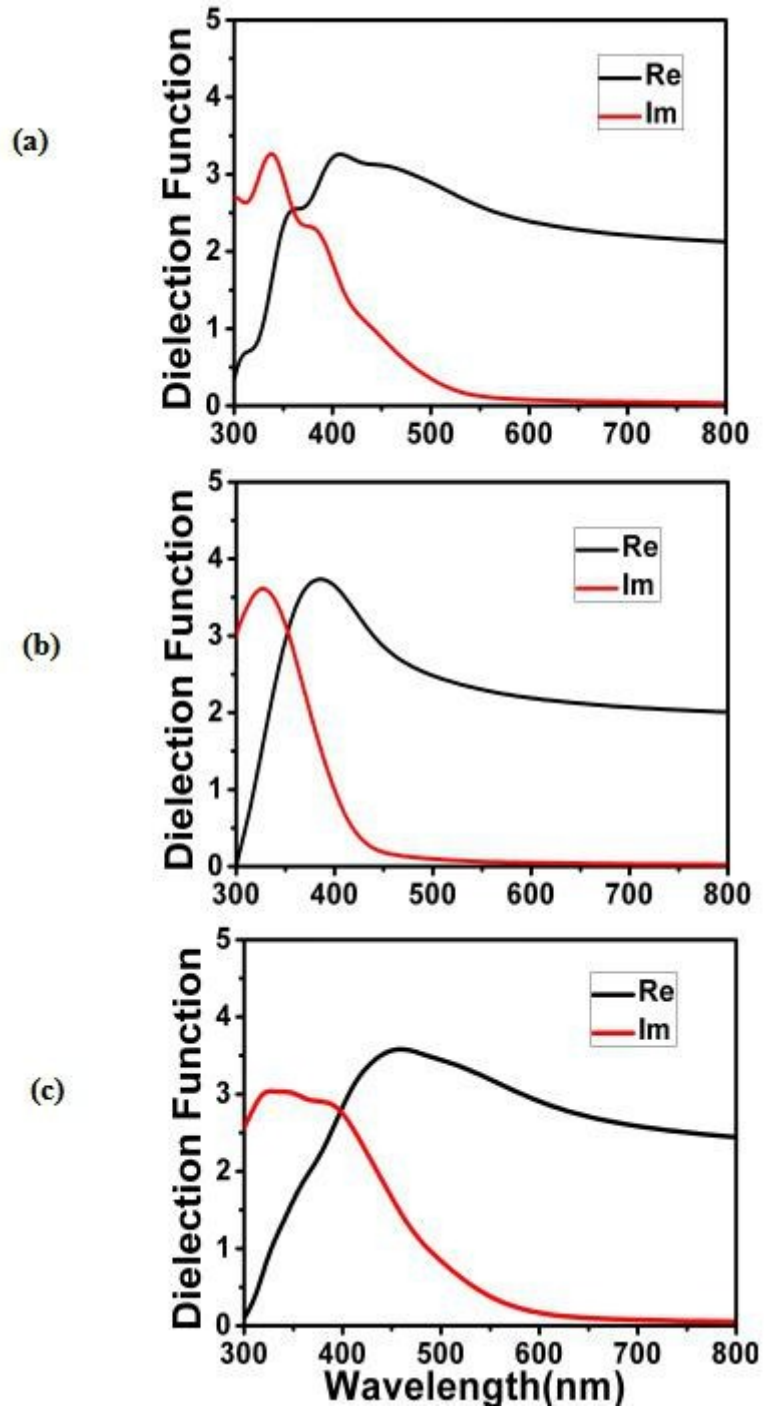


Figure S1. Calculated real and imaginary dielectric spectra of $\text{CH}_3\text{NH}_3\text{SnCl}_3$ perovskites (a) cubic, (b) monoclinic, (d) triclinic.

From the Figure S2, it shows that the shift of band edges as a function of strain along three directions of triclinic phase. Through dilating the lattice along the three directions, the DP constant E_1 is then calculated as $E_1 = \Delta E / (\Delta l / l_0)$ equivalent to the slope of the fitting lines, where E is the energy of the conduction (valence) band edge.

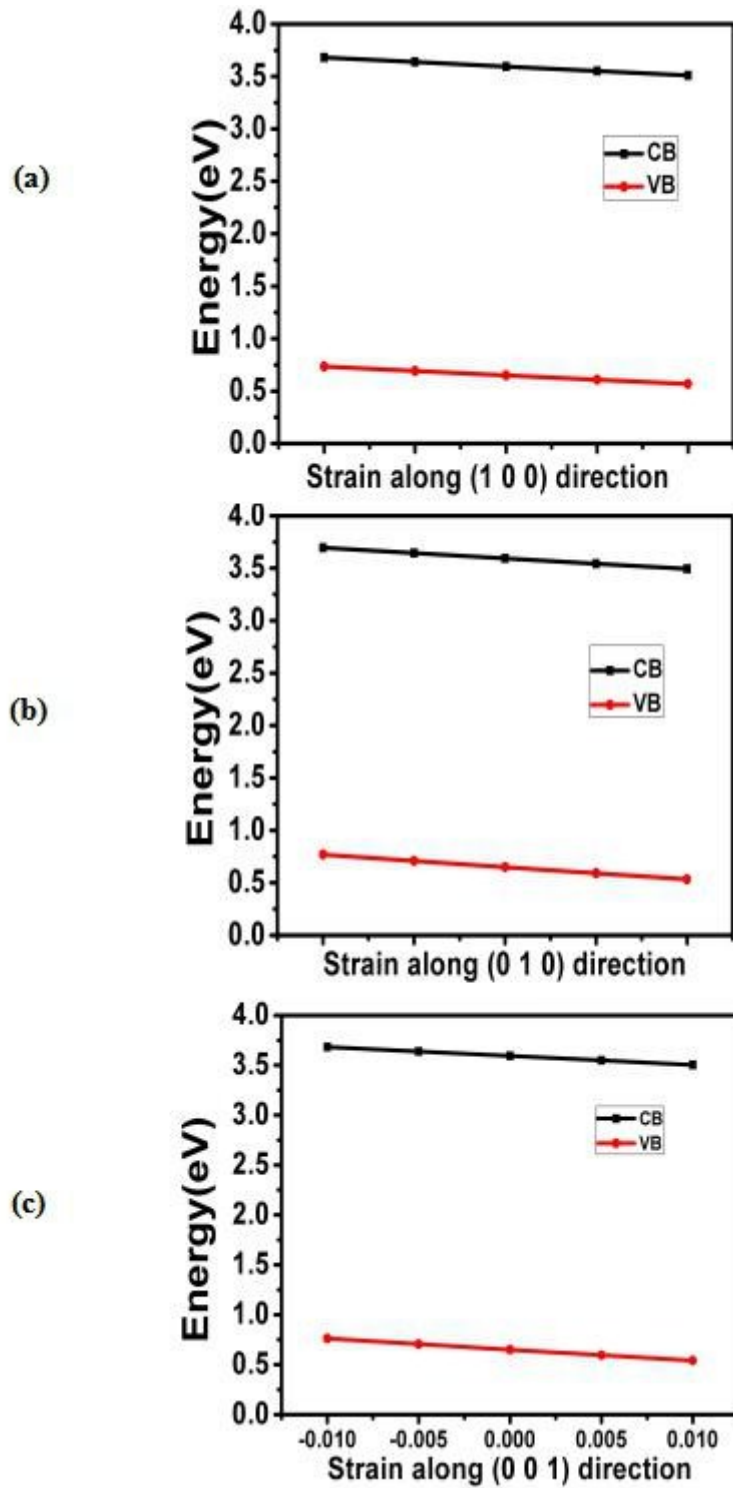


Figure S2. Calculated the band-edge positions of VB and CB with respect to the lattice dilation Δ/l_0 along the three direction for the triclinic phase of the $\text{CH}_3\text{NH}_3\text{SnCl}_3$. Solid liners represent the linear fit, which defines DP constant.

References:

- 1 J. Perdew, K. Burke and M. Ernzerhof, Generalized Gradient Approximation Made Simple. *Phys. Rev. Lett.* 1996, **77**, 3865-3868.
- 2 G. Kress and J. Hafner, Ab Initio Molecular Dynamics for Liquid Metals. *Phys. Rev. B* 1993, **47**, 558-561.
- 3 G. Kresse and J. Furthmüller, Efficient Iterative Schemes for ab initio Total-Energy Calculations Using a Plane-Wave Basis Set. *Phys. Rev. B* 1996, **54**, 11169-11186.
- 4 G. Kress And D. Jourbert, From ultrasoft pseudopotentials to the projector augmented-wave method. *Phys. Rev. B.* 1999, **59**, 1758.
- 5 H. J. Monkhorst and J. D. Pack, Special Points for Brillouin-Zone Integrations. *Phys. Rev. B.* 1976, **13**, 5188-5192.
- 6 K. Yamada, S. Fuanbiki, H. Horimoto, T. Matsui, T. Okuda, and S. Ichiba, Structural Phase Transitions of the Polymorphs of CsSnI₃ by Means of Rietveld Analysis of the X-Ray Diffraction. *Chem. Lett.* 2006, **20**, 801-804.